15th Canadian Masonry Symposium
Ottawa, Canada
June 2-5, 2025

Analysis Model for Slender Masonry Walls: The Effect of Wall-Foundation-Soil Interaction on the Out-Of-Plane Response

Alan Alonso[i], Mahmoud Elsayed[ii], Rafael Gonzalez[iii], Clayton Pettit[iv], Douglas Tomlinson[v], and Carlos Cruz-Noguez[vi]

ABSTRACT

Load-bearing masonry walls are an effective structural system for single-storey buildings such as warehouses, theatres, community centres, and school gymnasiums. Usually, these types of walls reach a height-to-thickness ratio greater than 30 and are subjected to combined gravity and lateral loads. Due to their perceived vulnerability to second-order effects, North American masonry design standards (CSA S304 and TMS 402/602) set additional design criteria for these walls. In the previous version of CSA S304-14, one of those design requirements was to assume a pinned base condition, neglecting the inherent stiffness provided by the wall-foundation-soil interaction, which affects the strength and stiffness of slender masonry walls. Current versions of CSA S304-24 and TMS 402/602-22 permit using a base support different of a pin for any height-to-thickness ratio by using a more comprehensive analysis. This study aims to determine the out-of-plane flexural response of masonry walls subjected to combined gravity and lateral loads under various height-to-thickness ratios, types of soils, footing geometry, and foundation depth. The parametric analysis showed increased flexural capacity and decreased deflections when the analysis included wall-foundation-soil interaction. The foundation depth and soil capacity were the aspects that most affected the base stiffness. Elastic effective height factors were proposed to account for base stiffness during the design of slender masonry walls for different values of rotational base stiffness. These findings imply that accounting for base stiffness in the analysis and design of slender masonry walls could be an untapped source of strength and stiffness, which may lead to more cost-effective masonry wall designs.

KEYWORDS

Base stiffness, foundation, masonry wall, out-of-plane, slender, soil-structure interaction

[i] Structural Engineer-in-Training, RCJ Engineers, Edmonton, Canada, aalonsorivers@rjc.ca
[ii] Ph.D. Candidate, University of Alberta, Edmonton, Canada, mhelsaye@ualberta.ca
[iii] Ph.D. Candidate, University of Alberta, Edmonton, Canada, rgonzalez@ualberta.ca
[iv] Assistant Professor, University of Alberta, Edmonton, Canada, cpettit@ualberta.ca
[v] Associate Professor, University of Alberta, Edmonton, Canada, dtomlinson@ualberta.ca
[vi] Professor, University of Alberta, Edmonton, Canada, cruznogu@ualberta.ca

INTRODUCTION

Tall load-bearing masonry walls are commonly used in low-rise buildings, such as industrial facilities, warehouses, retail establishments, and school gymnasiums. The flexural design of these walls is governed by a combination of moderate gravity loads and out-of-plane lateral loads. When the height-to-thickness (h/t) ratio exceeds 30, North American masonry design standards (CSA S304-24 [1] and TMS 402/602-22 [2]) imposed special design criteria due to their perceived vulnerability to second-order effects. The previous version of CSA S304 [3] mandated that designers neglect base stiffness despite the inherent stiffness provided by the wall-foundation-soil interaction. In contrast, TMS/602 402 [2, 4] permits using different types of base support for any h/t. The reluctance in the Canadian standard to account for the base stiffness may stem from the need for simplified and conservative design expressions before computers and specialized structural analysis software were more readily available and the lack of experimental data about the rapidly degrading wall-foundation interface under cyclic loading. The current version of CSA S304 [1] allows the designer to incorporate base stiffness through a comprehensive analysis which should include buckling effects, rotational support stiffness, and reinforcement detailing.

Since the 1980s, little innovation has occurred in slender masonry walls, when the American Concrete Institute (ACI) and the Structural Engineers Association of Southern California (SEASC) created a Test Report on Slender Walls [5], which influenced the subsequent Canadian masonry design standards [3, 6]. Later studies on masonry walls did not explore walls featuring other base conditions but only pin-end conditions [7–12] influenced by the ACI-ASEC [5] report. Few studies [13–17] have addressed the effect of base stiffness on the out-of-plane behaviour of masonry walls after the ACI-SEASC [5] report. Even though the studies related to base stiffness have demonstrated benefits of accounting for it, some important factors for the out-of-plane behaviour of slender walls have been neglected.

To overcome the economic, time, and practical constraints in experimental programs, numerical simulation has emerged as an excellent solution to provide reliable and cost-effective predictions of complex local [18–22] and global [23–29] behaviour of masonry structures. When the soil-structure interaction is included in the numerical simulation, similar approaches are used to model the soil domain. Depending on the level of detail of the required structural response, researchers opt to model the soil domain as a continuum [30–34] using a micro-modelling approach, while the macro-modelling approach is used more often to model the soil domain if the simplified model is enough for the required structural response. For instance, Pettit et al. [15, 16] captured the soil-foundation interaction by defining vertical springs along the foundation. However, the superstructure was neglected, and the springs were in the linear-elastic range.

This study aims to understand the effect of the wall-foundation-soil interaction in the out-of-plane flexural response of slender masonry walls by developing a finite-element macro model with static soil-structure interaction. A parametric analysis was performed, changing key parameters such as height-to-thickness ratios, types of soils, foundation geometry, and foundation depth. Results were analyzed in terms of flexural capacity, base stiffness intensity, and stability analysis to propose effective height factors (k) for different foundation conditions.

TYPICAL CONFIGURATION OF SLENDER MASONRY WALLS

Slender masonry walls in single-storey buildings typically range from 4 to 8 metres. Moderate gravity loads and small inertial forces are expected when light roof systems are used. However, wind loads can be critical due to the large spans and exposed areas in the out-of-plane direction. The design of these types of walls is governed by flexure due to the combined effects of gravity and out-of-plane loads. To resist the combined effects of gravity and out-of-plane loads, a vertical reinforcement configuration and grout scheme are selected when designing these types of walls. To optimize the structural design, engineers often prefer partially grouted (PG) walls over fully grouted (FG) walls to reduce self-weight and second-order effects. Reducing the gravity load transmitted to the soil enables the use of strip footings when the soil is moderately competent. Strip footings are complemented by foundation walls which, in masonry construction, can be FG from the footing to the ground level. The connection between the wall and the foundation is made by dowels fully anchored into the footing and spliced with the flexural steel reinforcement at the bottom of the wall. Based on the description of a typical configuration of slender masonry walls, Figure 1 shows the characteristics considered in terms of loading, reinforcing, and wall-foundation connection in the analysis model.

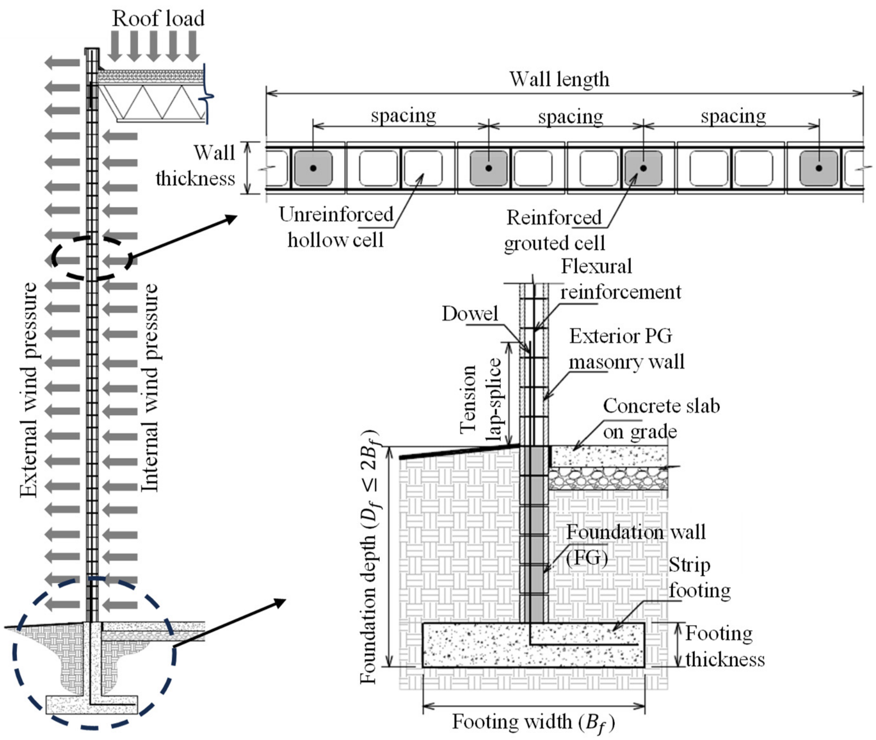

Figure 1: Typical Loading, Reinforcing Configuration, and Foundation Connection

ANALYSIS MODEL

Numerical Model

The model was developed using displacement-based beam-column type elements in an open-source FE software framework OpenSees [35]. A fibre cross-section was used to capture the material nonlinearity through distributed plasticity. The homogenous behaviour of the masonry assemblage was simulated using the material C*oncrete02* based on the Kent-Scott-Park model [36]. The steel reinforcement was simulated using the material *Steel02* with isotropic strain hardening based on the Guiffre-Menogoto-Pinto model [37]. A *hysteretic* material model available in the OpenSees library was used to implement the modified stress-strain behaviour of the steel in lap splice, based on the model proposed by Barkhordary and Tariverdilo [38]. The geometric nonlinearity was considered by implementing the *Corotational* geometric transformation rule in the OpenSees library. The top of the wall is free in the global Y direction but restrained in the global X direction while allowing rotation emulating roller support. The model was divided into two modules to simulate the base of the wall. Module 1 consisted of simplified base conditions (pinned, partially fixed, or fixed), while Module 2 explicitly modelled the soil-foundation interaction by using the beam-on-nonlinear-Winkler-foundation (BNWF) method [39, 40]. Elastic beam-column elements were used to model the footing, while the nonlinear properties of the soil were modelled using zero-length soil elements (q-z, p-y, and t-z). The static vertical and lateral stiffness of the soil was obtained using the equations proposed by Gazetas [41] and Mylonakis et al. [42]. Loading-wise, the macro model described was analyzed using a monotonic push-over analysis. The vertical axial load (P) with eccentricity (e) was modelled by the equivalent axial load and moment combination ($P,\ M = P \cdot e$) while the self-weight was applied uniform distributed along the height of the wall. The lateral pressure (ω) is applied along the height of the wall until the target displacement at midspan is achieved. The schematic drawing of the model described is shown in Figure 2 while details of the soil-foundation interaction implemented in Module 2 are shown in Figure 3.

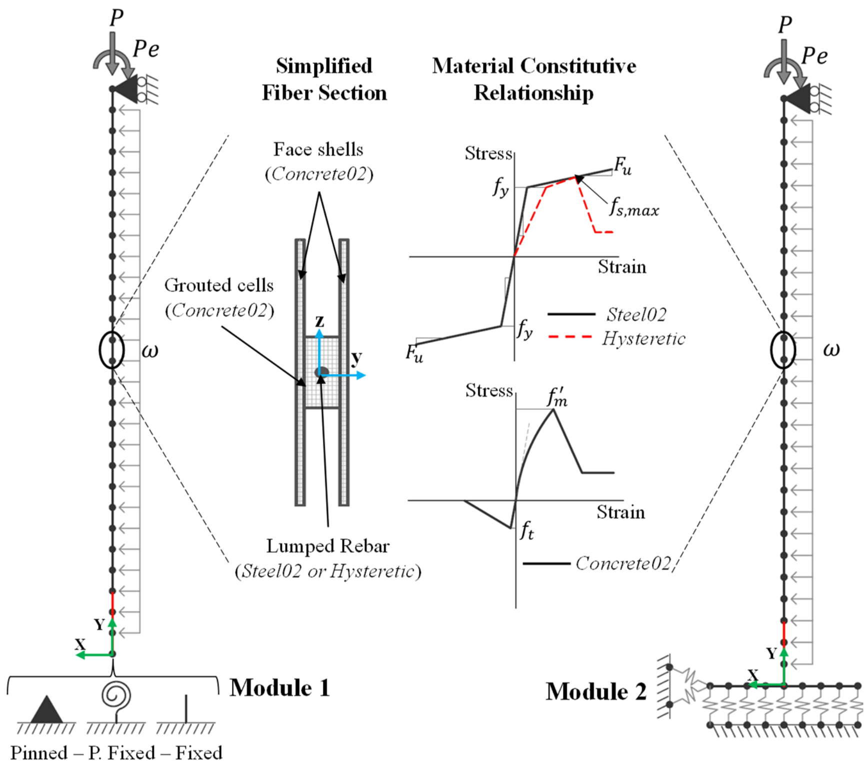

Figure 2: Finite Element macro model composition (global axes: green; local axes: blue)

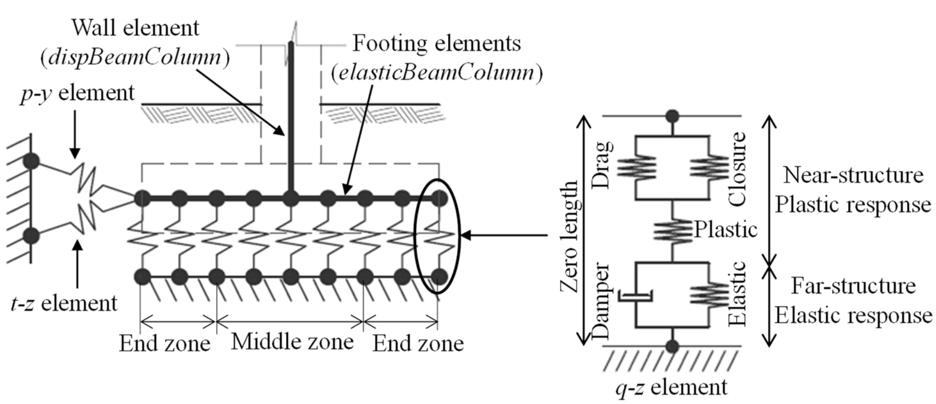

Figure 3: Beam-on-Nonlinear-Winkler-Foundation (BNWF) model used in Module 2

Model Validation

Results from the experimental testing by Alonso et al. [17] were used to validate the model. The experimental program consisted of two full-scale, partially grouted walls, tested under combined eccentric axial load and out-of-plane pressure. The walls were 8750 mm high, 1190 mm wide, and 190 mm thick, with h/t = 46. The vertical reinforcement consists of 2-15M (area of 200 mm^2 each) bars at 600 mm. Figure 4 compares the experimental load-displacement history from Wall-1 and -2 with the predicted capacity curve from the numerical model. Figure 5 compares the tensile (steel) and compressive (block) strains predicted in the numerical model with the strains captured during the test where maximum moments were located. The results show that the numerical model achieved reasonable agreement in the global (predicted out-of-plane capacity) and local (predicted strains at critical locations) response compared with the experimental results of both walls tested under different base conditions.

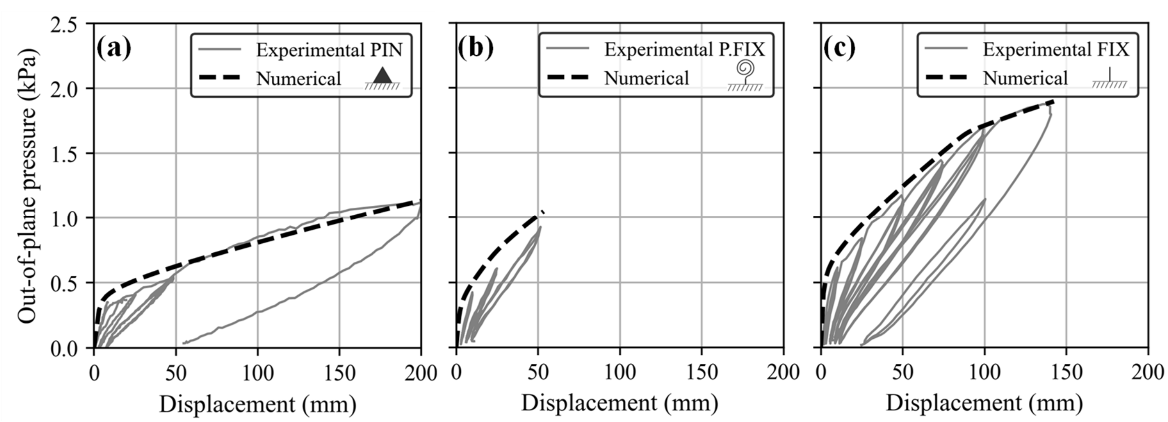

Figure 4: Model Validation – Global Response: (a) Wall-1 (pinned base); (b) Wall-2 (partially fixed base); (c) Wall-2 (fixed base)

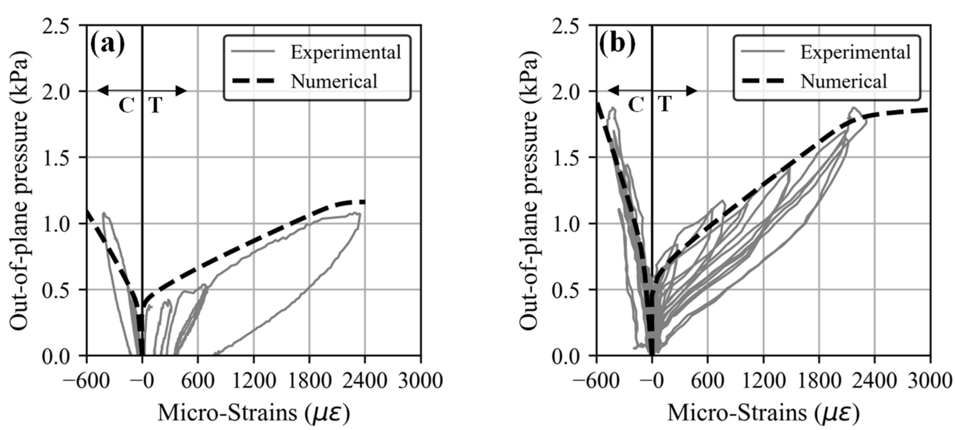

Figure 5: Model Validation – Local Response: (a) Strains at midspan in Wall-1 (pinned base); (b) Strains at wall base in Wall-2 (fixed base)

Model Limitations

- The model does not include out-of-plane shear failure mechanisms since walls with heights > 3.0 m are flexure dominated, which is the primary focus of this research. If short walls are analyzed, shear failure mechanisms must be included.

- The model cannot predict detailed local responses such as crack propagation, material degradation, or join openings. A micro-modelling approach is recommended when detailed analyses are required.
- The model does not account for dynamic loading or material degradation. For dynamic loading, material models must incorporate degradation parameters and soil stiffness must be adjusted using frequency-dependent dynamic factors.

PARAMETRIC STUDY

Fixed, Dependent, and Independent Parameters

Table 1 summarizes the fixed parameters that did not vary during the study. The walls analyzed were PG with 15 MPa–20cm concrete masonry units (CMU) and reinforced with 15M bars every 600 mm. The total axial load maintained a constant ratio of 0.9 with the maximum axial load allowed ($0.05f'_mA_e$) by the TMS 402/406 [2] during the analyses. The out-of-plane capacity of the loadbearing-slender masonry walls and the equivalent rotational base stiffness (RBS) were the dependent parameters of this study. These parameters were obtained from different cases of slenderness ratio, soil type, foundation depth, and footing width. Table 2 summarizes the independent parameters, such as wall height (h), soil type (Table 3), foundation depth (D_f), and footing width (B_f), were selected to investigate the effect on the dependent parameters. The height of the walls varied according to the usual range found in single-storey buildings, modifying the h/t ratio, the initial imperfection at midspan ($0.1h$), and the self-weight of the wall (P_w). The maximum foundation depth used in the analysis was 1.20 m – the minimum depth recommended for shallow foundations from frost heaving in cold climates.

Table 1: Fixed Parameters

Parameter	Value
Wall thickness	190 mm
Wall effective width	1000 mm
Total axial load ($P_f = P + P_w$)	40 kN/m
Load eccentricity (e)	63 mm
Compressive Masonry Strength (f'_m)	8.5 MPa
Tensile Masonry Strength (f_t)	0.55 MPa
Effective area of steel per metre (A_{s_m})	333 mm2/m
Steel Yield Strength (f_y)	400 MPa
Steel Modulus of Elasticity (E_s)	200 GPa

Table 2: Simulation Matrix

Parameter	Values
Wall height (h)	[4.8, 5.8, 6.8, 7.6] m
External axial load (P)	[31, 29, 26, 22] kN/m
Soil type: Sand	[Loose, Medium, Dense]
Soil type: Clay	[Soft, Medium, Stiff]
Foundation depth (D_f)	[0.30, 0.60, 0.90, 1.20] m
Footing width (B_f)	[0.60 – 1.60] every 0.10 m

Table 3: Typical Soil Classification and Properties [43]

Type of soil		Unit Weight (kN/m³)	Internal friction angle (degrees)	Cohesion (kPa)	Poisson's ratio	Modulus of Elasticity (MPa)
Sand	Loose	14.5	28	-----	0.30	20
	Medium	16.5	32	-----	0.33	25
	Dense	18.0	37	-----	0.38	45
Clay	Soft	11.5	-----	25	0.35	12
	Medium	14.5	-----	50	0.35	30
	Stiff	17.0	-----	100	0.35	70

RESULTS AND DISCUSSION

Load-Displacement Curves

Load-displacement curves were obtained to evaluate the effect of the slenderness ratio (h/t), foundation depth (D_f), and footing width (B_f) in the wall capacity for each type of soil. The lateral pressure (LP) and lateral displacement at midspan (Δ_{mid}) were normalized with the maximum lateral pressure (LP_{max}) and wall height (h) obtained from the fixed base condition, respectively. It can be noticed in Figure 6 how accounting for the wall-foundation interaction increases the out-of-plane capacity of walls and it is more significant as the wall becomes more slender. For instance, when the wall was simulated with B_f= 0.60 m, D_f= 0.60 m, the out-of-plane capacity increased by 41% for loose sand and 50% for soft clay for walls with a $h/t = 25$ while the increment was by 100% for loose sand and 126% for soft clay for walls with a $h/t = 40$, compared with the pinned base scenario.

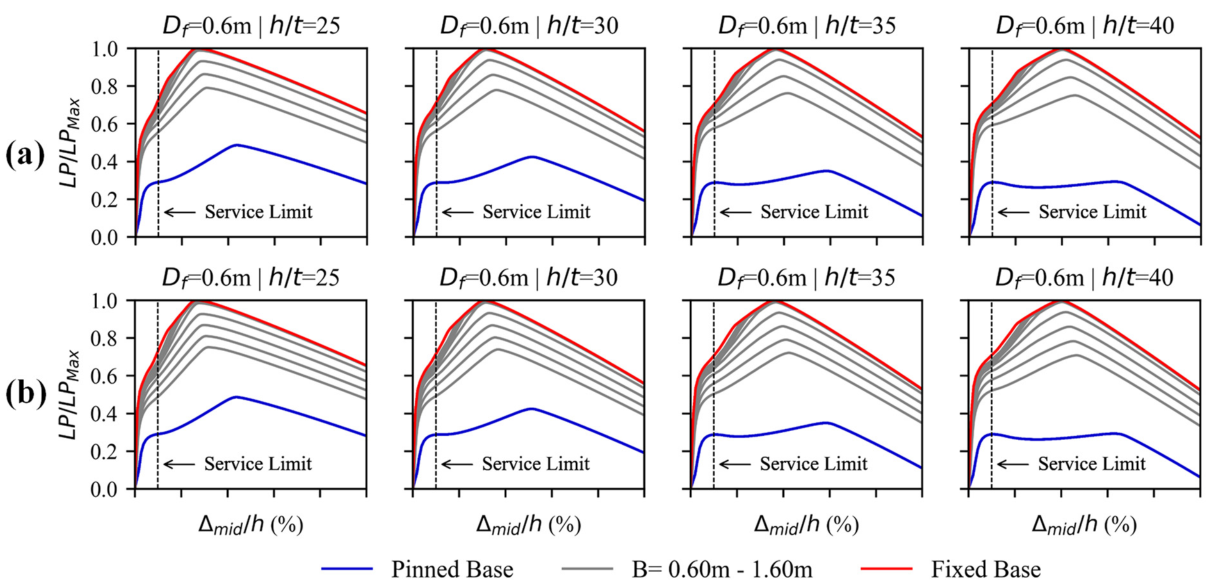

Figure 6: Load-Displacement Curves: (a) Loose Sand; (b) Soft Clay

Base Rotation Intensity and Equivalent Rotational Base Stiffness

The level of fixity provided by the wall-foundation interaction can be observed in Figure 7, the closer the rotation ratio (θ/θ_{max}) is to zero, the base will tend to behave as a fixed condition, while if θ/θ_{max} is closer to one, the base will tend to behave as a pinned condition. For example, the base can be considered as pinned within D_f/h and $B_f/h \leq 0.1$, as partially fixed within $D_f/h > 0.1$ and $0 < B_f/h \leq 0.1$, and as fixed within D_f/h and $B_f/h > 0.1$.

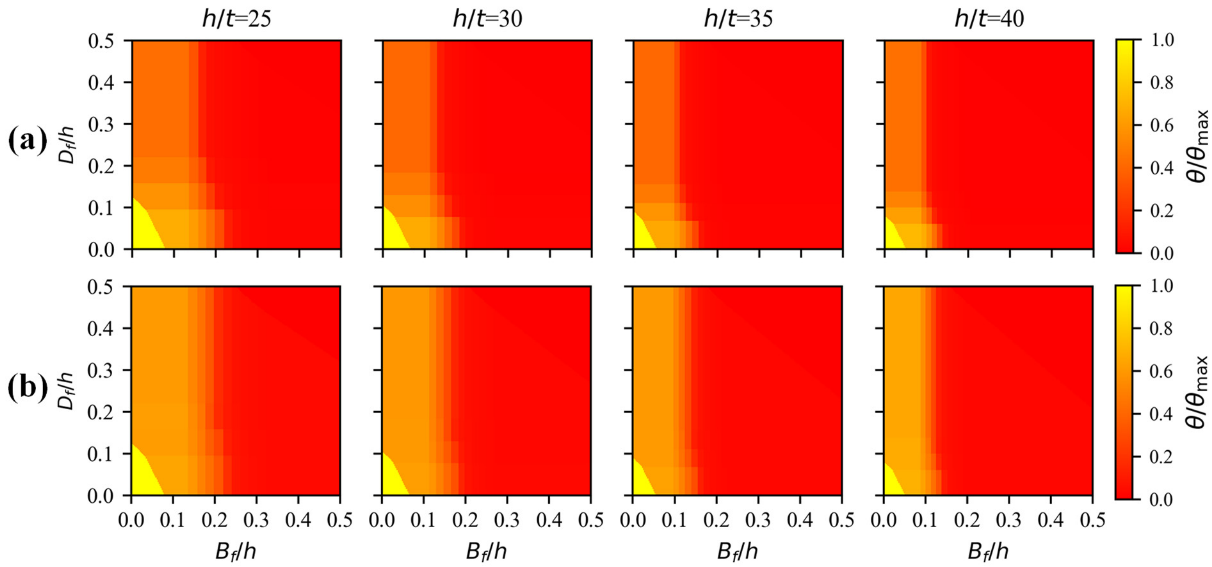

Figure 7: Base Rotation Intensity: (a) Loose Sand; (b) Soft Clay

The equivalent rotational base stiffness (*RBS*) is a more practical interpretation of the base rotation intensity. Table 4 and 5 show the range of equivalent *RBS* values from different h/t ratios (25, 30, 35, and 40) obtained by using Eq.(1). Where M_b is the base moment and θ is the base rotation at the maximum lateral pressure.

(1) $$RBS = \frac{M_b}{\theta}$$

Table 4: Equivalent Rotational Base Stiffness (RBS) on Sand

D_f (m)	B_f (m)	Loose	Medium	Dense
			RBS (kN-m/rad)	
0.3	0.6	80 – 95	200 – 290	320 – 460
0.3	0.8	210 – 300	530 – 730	1,500 – 2,260
0.3	1.0	720 – 840	4,800 – 5,600	40,600 – 41,550
0.3	1.2	4,600 – 5,300	14,000 – 14,960	56,200 – 56,400
0.6	0.6	170 – 250	300 – 430	420 – 600
0.6	0.8	490 – 650	1,300 – 1,780	10,400 – 19,950
0.6	1.0	3,000 – 3,400	9,800 – 10,600	43,600 – 44,050
0.6	1.2	7,250 – 7,500	24,800 – 26,600	56,800 – 56,900
0.9	0.6	250 – 400	350 – 550	510 – 700
0.9	0.8	950 – 1,170	3,800 – 4,850	28,800 – 30,550
0.9	1.0	5,200 – 5,500	17,800 – 19,600	45,250 – 45,450
0.9	1.2	8,700 – 9,070	28,350 – 28,500	57,200 – 57,250
1.2	0.6	360 – 500	490 – 660	700 – 870
1.2	0.8	2,100 – 2,500	8,500 – 9,500	32,300 – 33,100
1.2	1.0	6,250 – 6,500	22,100 – 22,250	45,800 – 45,900
1.2	1.2	11,700 – 12,300	28,800 – 28,900	57,500 – 57,550

Table 5: Equivalent Rotational Base Stiffness (RBS) on Clay

D_f (m)	B_f (m)	Soft	Medium	Stiff
			RBS (kN-m/rad)	
0.3	0.6	110 – 150	250 – 370	350 – 520
0.3	0.8	240 – 340	640 – 860	2,700 – 4,100
0.3	1.0	580 – 750	8,500 – 8,900	23,200 – 23,800
0.3	1.2	3,120 – 3,450	12,850 – 13,000	32,900 – 33,150
0.6	0.6	140 – 200	300 – 450	430 – 600
0.6	0.8	300 – 410	1,800 – 3,000	8,300 – 12,000
0.6	1.0	950 – 1,250	9,300 – 9,520	24,650 – 24,950
0.6	1.2	3,450 – 3,700	12,900 – 13,000	32,750 – 33,000
0.9	0.6	140 – 190	350 – 500	500 – 700
0.9	0.8	340 – 450	4,200 – 5,350	15,500 – 16,550
0.9	1.0	1,650 – 1950	9,700 – 9,850	25,200 – 25,500
0.9	1.2	3,800 – 4,000	13,000 – 13,150	33,050 – 33,300
1.2	0.6	150 – 200	390 – 570	650 – 850
1.2	0.8	400 – 480	5,750 – 6,150	17,150 – 17,650
1.2	1.0	1,500 – 1,800	9,700 – 9,850	25,200 – 25,350
1.2	1.2	4,050 – 4,200	13,150 – 13,250	33,350 – 33,600

Stability Analysis and Elastic Effective Height Factors (*k*)

Stability analysis was performed on slender masonry walls with different h/t ratios (25, 30, 35, and 40) by using Module 1 of the analysis model. The partially fixed condition was simulated using the lower bounds of RBS from Table 4-5 with an initial imperfection of $0.1h$ at midspan, and an increasing concentric axial load (P) was applied at the top of the wall until elastic buckling failure was reached. The load at the elastic buckling failure with an end-restrained is known as elastic critical load (P_{cr}), while the load at the elastic buckling failure under pin-end conditions is known as the Euler buckling load (P_e) and can be obtained by Eq. (2). Using P_{cr} and P_e the elastic effective height factors can be calculated by Eq. (3).

(2) $$P_e = \frac{\pi^2 E_m I_{cr}}{h^2}$$

(3) $$k = \sqrt{\frac{P_e}{P_{cr}}}$$

Where E_m is the modulus of elasticity of the masonry assembly, I_{cr} is the cracked moment of inertia, and h is the height of the wall.

Table 6 shows a summary of the elastic effective height factors (k) obtained for different height-to-thickness ratios (h/t) with different ranges of RBS values. The elastic effective height factor calculated ($k_{calculated}$) can not be used directly for design since ideal conditions are rarely achieved in practice. Therefore, the elastic effective height factors proposed ($k_{proposed}$) were increased by 10% to account for uncertainties such as workmanship (out-of-plumbness, reinforcement location, etc.), the position of the loads, variability of material strength, and degradation due to the life cycle of the structure. However, a reliability analysis (out of the scope of this study) is recommended to accurately account for the uncertainties previously mentioned.

Table 6: Elastic Effective Height Factors (k)

h/t	RBS (kN-m/rad)	$k_{calculated}$	$k_{proposed}$
25	80 – 150	0.9	1.0
25	170 – 650	0.8	0.9
25	> 700	0.7	0.8
30	80 – 110	0.9	1.0
30	150 – 530	0.8	0.9
30	> 580	0.7	0.8
35	80	0.9	1.0
35	110 – 360	0.8	0.9
35	> 420	0.7	0.8
40	80	0.9	1.0
40	110 – 360	0.8	0.9
40	> 420	0.7	0.8

CONCLUSIONS

This study developed an analytical model to investigate the impact of wall-foundation-soil interaction on the out-of-plane response of slender masonry walls. A parametric analysis was conducted by varying key parameters, including wall height, soil type, foundation depth, and footing width. Based on the findings, elastic effective height factors (k) were proposed, leading to the following conclusions:

- Wall-foundation-soil interaction is an untapped source of stiffness that enhances the performance of load-bearing masonry walls, increasing the out-of-plane capacity while reducing displacements.
- The increase in capacity is attributed to the change of moment distribution along the wall height, influenced by the presence of base stiffness, which is inversely proportional to the base rotation.
- Base rotation is mainly affected by the foundation depth and the bearing capacity of the soil.
- The benefit of accounting for base stiffness relies on the effective moment connection between the wall and the foundation, which facilitates stress distribution into the soil creating a semi-rigid base condition.
- The application of elastic effective height factors can be an alternative for designers to account for base stiffness in slender masonry wall design, reducing the impact of assuming a pinned base.

While this study demonstrates the benefits of wall-foundation-soil interaction under monotonic loading and strip footings, further research is needed to evaluate the behaviour of the wall-foundation connection under dynamic loading conditions. Investigating potential degradation mechanisms will help determine whether the level of fixity remains consistent until failure.

ACKNOWLEDGEMENTS

The authors wish to acknowledge the generous contribution, both monetary and in kind, from the Masonry Contractor Association of Alberta (MCAA), the Canada Masonry Design Centre (CMDC), the Canadian Masonry Producers Association (CCMPA), the National Council of Science and Technology of Mexico (CONACYT), and Read Jones Christoffersen Ltd. (RJC Engineers).

REFERENCES

[1] (CSA) Canadian Standards Association, "Design of masonry structures. Standard CSA S304-24," CSA Group, Rexdale, ON, 2024.

[2] (TMS) The Masonry Society, "TMS 402/602-22 Building code requirements and specification for masonry structures," MJSC, Longmont, CO, 2022.

[3] (CSA) Canadian Standards Association, "Design of masonry structures. Standard CSA S304-14 (R2019)," CSA Group, Rexdale, ON, 2019.

[4] (TMS) The Masonry Society, "TMS 402/602-16 Building code requirements and specification for masonry structures," MJSC, Longmont, CO, 2016.

[5] ACI-SEASC Task Committee on Slender Walls, "Test Report on Slender Walls," ACI-SEASC (American Concrete Institute - Structural Engineers Association of Southern California), Sep. 1982.

[6] (CSA) Canadian Standards Association, "Design of Masonry Structures. Standard CSA S304.1-M94," CSA Group, Rexdale, ON, 1994.

[7] Y. Liu, G. G. Aridru, and J. L. Dawe, "Effective Flexural Rigidity of Concrete Masonry Walls," in *8th Canadian Masonry Symposium*, Jasper, AB. Canada, 1998, pp. 18–24.

[8] Y. Liu and J. L. Dawe, "Experimental determination of masonry beam-column behaviour," *Can. J. Civ. Eng.*, vol. 28, no. 5, pp. 794–803, 2001.

[9] Y. Liu and K. Hu, "Experimental study of reinforced masonry walls subjected to combined axial load and out-of-plane bendingThis article is one of a selection of papers published in this Special Issue on Masonry," *Can. J. Civ. Eng.*, vol. 34, no. 11, pp. 1486–1494, Nov. 2007.

[10] J. R. Bean Popehn, A. E. Schultz, M. Lu, H. K. Stolarski, and N. J. Ojard, "Influence of transverse loading on the stability of slender unreinforced masonry walls," *Eng. Struct.*, vol. 30, no. 10, pp. 2830–2839, Oct. 2008.

[11] A. Sparling, D. Palermo, and F. Hashemian, "Out-of-plane flexural testing and stiffness response of concrete masonry walls with NSM steel reinforcement," *Can. J. Civ. Eng.*, no. cjce-2019-0685, pp. 1–14, Jun. 2020.

[12] A. Sparling and D. Palermo, "Response of full-scale slender masonry walls with conventional and NSM steel reinforcement subjected to axial and out-of-plane loads," *J. Struct. Eng.*, vol. 149, no. 1, p. 04022208, Jan. 2023.

[13] E. Mohsin, "Support Stiffness Effect on Tall Load Bearing Masonry Walls," PhD, University of Alberta, 2005.

[14] A. C. Isfeld, A. L. Müller, M. Hagel, and N. G. Shrive, "Analysis of safety of slender concrete masonry walls in relation to CSA S304-14," *Can. J. Civ. Eng.*, vol. 46, no. 5, pp. 424–438, May 2019.

[15] C. Pettit and C. Cruz-Noguez, "Effect of Rotational Base Stiffness on the Behavior of Load-Bearing Masonry Walls," *J. Struct. Eng.*, vol. 147, no. 12, p. 04021215, Dec. 2021.

[16] C. Pettit, E. Mohsin, C. Cruz-Noguez, and A. Elwi, "Experimental testing of slender load-bearing masonry walls with realistic support conditions," *Can. J. Civ. Eng.*, vol. 49, no. 1, pp. 95–108, Jan. 2022.

[17] A. Alonso *et al.*, "Experimental testing of tall slender masonry walls with different rotational base stiffnesses," *J. Struct. Eng. (N. Y.)*, vol. 150, no. 3, Mar. 2024.

[18] A. W. Page, "Finite Element Model for Masonry," *Journal of the Structural Division*, vol. 104, no. 8, pp. 1267–1285, Aug. 1978.

[19] S. Ali, A. Page, and P. W. Kleeman, "Non-Linear Finite Element Model for Concrete Masonry with Particular Reference to Concentrated Loads," in *4th Canadian Masonry Symposium*, New Brunswick, CA, 1986, pp. 137–148.

[20] H. R. Lotfi and P. B. Shing, "Interface Model Applied to Fracture of Masonry Structures," *J. Struct. Eng.*, vol. 120, no. 1, pp. 63–80, 1994.

[21] E. Y. Sayed-Ahmed and N. G. Shrive, "Numerical analysis of face-shell bedded hollow masonry walls subject to concentrated loads," *Can. J. Civ. Eng.*, vol. 22, no. 4, pp. 802–818, Aug. 1995.

[22] J. Yi and N. G. Shrive, “3D Finite Element Models of Plain and Bond-Beamed Hollow Masonry Walls Subjected to Concentric and Eccentric Concentrated Loads,” in *9th Canadian Masonry Symposium*, Fredericton, NB, Canada, 2001.
[23] R. Wang, A. E. Elwi, M. A. Hatzinikolas, and J. Warwaruk, “Test of Tall Cavity Walls Subjected to Eccentric Loading,” *J. Struct. Eng.*, vol. 123, no. 7, pp. 912–919, 1997.
[24] J. Lopez, S. Oller, E. Onate, and J. Lubliner, “A Homogeneous Constitutive Model for Masonry,” *Int. J. Numer. Meth. Engng.*, vol. 46, pp. 1651–1671, 1999.
[25] R. R. van der Pluijm, “Out-of-plane bending of masonry: behaviour and strength,” PhD, Eindhoven University of Technology, 1999.
[26] G. Ma, H. Hao, and Y. Lu, “Homogenization of Masonry Using Numerical Simulations,” *J. Eng. Mech.*, vol. 127, no. 5, pp. 421–431, 2001.
[27] M. Donà, G. Tecchio, and F. da Porto, “Verification of second-order effects in slender reinforced masonry walls,” *Mater. Struct.*, vol. 51, no. 3, p. 69, May 2018.
[28] A. Alonso, R. Gonzalez, C. Cruz-Noguez, and D. Tomlinson, “Pre-Test Analysis of The Effect of Rotational Base Stiffness on Loadbearing Slender Masonry Walls,” in *14th Canadian Masonry Symposium*, Montreal, QC, 2021.
[29] Z. Metwally, B. Zeng, and Y. Li, “Probabilistic Behavior and Variance-Based Sensitivity Analysis of Reinforced Concrete Masonry Walls Considering Slenderness Effect,” *ASCE-ASME J. Risk and Uncertainty Eng. Syst., Part A: Civ. Eng.*, vol. 8, no. 4, p. 04022051, Dec. 2022.
[30] Masia Mark J., Kleeman Peter W., and Melchers Robert E., “Modeling Soil/Structure Interaction for Masonry Structures,” *J. Struct. Eng.* , vol. 130, no. 4, pp. 641–649, Apr. 2004.
[31] H. Güllü and H. S. Jaf, “Full 3D nonlinear time history analysis of dynamic soil–structure interaction for a historical masonry arch bridge,” *Environ. Earth Sci.*, vol. 75, no. 21, p. 1421, Nov. 2016.
[32] A. Piro, F. de Silva, F. Parisi, A. Scotto di Santolo, and F. Silvestri, “Effects of soil-foundation-structure interaction on fundamental frequency and radiation damping ratio of historical masonry building sub-structures,” *Bull. Earthquake Eng.*, vol. 18, no. 4, pp. 1187–1212, Mar. 2020.
[33] F. de Silva, “Influence of soil-structure interaction on the site-specific seismic demand to masonry towers,” *Soil Dynamics and Earthquake Engineering*, vol. 131, p. 106023, Apr. 2020.
[34] A. Fathi, A. Sadeghi, M. R. Emami Azadi, and N. Hoveidae, “Assessing the soil-structure interaction effects by direct method on the out-of-plane behavior of masonry structures (case study: Arge-Tabriz),” *Bull. Earthquake Eng.*, vol. 18, no. 14, pp. 6429–6443, Nov. 2020.
[35] F. McKenna, M. H. Scott, and B. Jeremic, “Open System for Earthquake Engineering Simulation (OpenSees) [Computer Software],” Pacific Earthquake Engineering Research Centre, University of California Berkley, California, USA., 2000.
[36] D. C. Kent and R. Park, “Flexural members with confined concrete,” *Journal of the Structural Division*, vol. 97, no. 7, pp. 1969–1990, Jul. 1971.
[37] M. Menegotto and P. E. Pinto, “Method of analysis for cyclically loaded reinforced concrete plane force and bending,” *Proceedings, IABSE Symposium on Resistance and*, 1973.
[38] M. Barkhordary and S. Tariverdilo, “Vulnerability of ordinary moment resistant concrete frames,” *Earthquake Engineering and Engineering Vibration*, vol. 10, no. 4, pp. 519–533, Dec. 2011.
[39] C. W. Harden and T. C. Hutchinson, “Beam-on-Nonlinear-Winkler-Foundation Modeling of Shallow, Rocking-Dominated Footings,” *Earthquake Spectra*, vol. 25, no. 2, pp. 277–300, May 2009.
[40] C. Harden, T. Hutchinson, G. R. Martin, and B. L. Kutter, “Numerical Modeling of the Nonlinear Cyclic Response of Shallow Foundations,” Pacific Earthquake Engineering Research (PEER) Center, Aug. 2005.
[41] G. Gazetas, “Formulas and Charts for Impedances of Surface and Embedded Foundations,” *ASEC - J. Geotech. Engrg.*, vol. 117, no. 9, pp. 1363–1381, Sep. 1991.
[42] G. Mylonakis, S. Nikolaou, and G. Gazetas, “Footings under seismic loading: Analysis and design issues with emphasis on bridge foundations,” *Soil Dynamics and Earthquake Engineering*, vol. 26, no. 9, pp. 824–853, Sep. 2006.
[43] B. M. Das, *Principles of foundation engineering*. Cengage Learning, 2023.